J Electroceram (2008) 21:478–481
DOI 10.1007/s10832-007-9224-1

The sintering behavior and microwave dielectric properties of $Mg_4(Nb,Sb)_2O_9$ ceramics

P. Liu · W.A. Su · G.G. Yao · X.B. Bian

Published online: 13 September 2007
© Springer Science + Business Media, LLC 2007

Abstract The sintering behavior, microstructure and microwave dielectric properties of $Mg_4(Nb_{2-x}Sb_x)O_9$ ($0 \le x \le 2$) solid solutions were investigated systematically by X-ray diffraction(XRD), scanning electron microscopy(SEM) and a network analyzer. The solid solutions of $Mg_4(Nb_{2-x}Sb_x)O_9$ was formed with x value being no more than 1.6. The dielectric constant (ε) of the sintered ceramics decreased from 13.06 to 6.28 with Sb content x from 0 to 1.6. With a substitution of Sb^{5+} for Nb^{5+} ($0.04 \le x \le 0.08$), the sintering temperature of $Mg_4Nb_2O_9$ ceramics was decreased from 1400 to 1300 °C without degradation of the Qf values. The optimum microwave dielectric properties of $\varepsilon \sim 12.26$, Qf~ 168,450 GHz, and $\tau_f \sim -56.4$ ppm/°C were obtained in the composition of $Mg_4(Nb_{1.6}Sb_{0.4})O_9$ sintered at 1300 °C.

Keywords Microwave dielectric ceramic · $Mg_4(Nb_{2-x}Sb_x)O_9$ · High Q · Low ε value · Magnesium niobate

1 Introduction

The development of high Q materials with a variety of dielectric constant, ε, is essential in the advancement of wireless communication industry. Thus, a number of these materials have been investigated and developed [1–5]. Among which, α-Al_2O_3 ceramics with corundum structure has a very high Q value (Qf~300,000 GHz) and low dielectric constant ($\varepsilon \sim 10$), widely used as substrate and IC packaging materials. Very recently, it was found that $Mg_4Nb_2O_9$ (MN) ceramics exhibited a very high Qf value comparable to Al_2O_3[6]. By a substitution of Ta^{5+} for Nb^{5+}, the Qf value of $Mg_4Nb_2O_9$ could be further improved [6]. Thus, $Mg_4Nb_2O_9$ is a suitable material for microwave applications, such as substrates and resonators at high frequency. In this work, $Mg_4(Nb_{2-x}Sb_x)O_9$ ($0 \le x \le 2$) solid solutions were fabricated by a conventional solid reaction method and the sintering behavior, microstructures, and microwave dielectric properties of $Mg_4(Nb_{2-x}Sb_x)O_9$ ceramics were investigated.

2 Experiment procedure

Samples of $Mg_4(Nb_{2-x}Sb_x)O_9$ ($0 \le x \le 2$) were prepared by standard electronic ceramic method. The starting materials were oxide powders: high purity MgO (≥99.9%), Nb_2O_5 (≥99.5%) and analysis grade Sb_2O_5 (≤99.0%). The powders were weighed according to the stoichiometric ratio and then milled in a polyethylene bottle with agate balls for 10 h using alcohol as a medium. Mixtures were dried and calcined at 1000 °C for 10 h. The calcined powders were re-milled for 10 h, then ground with PVA solution as a binder and sieved through a 60-mesh screen. Pellets with 15 mm in diameter and 7 mm in thickness were pressed using uniaxial pressing. These pellets were subsequently sintered at 1300–1400 °C for 5 h in air.

The crystalline phases were analysed by X-ray powder diffraction (XRPD, Rigaku D/max 2550, Japan) using Cu Kα radiation (at 40 Kv and 200 mA) of 2θ from 10° to 80°. The surface microstructure of the as-sintered ceramics were observed by a scanning electron microscopy (Quanta 200 SEM, Holland). The bulk density (ρ) of the sintered pellets was measured by the Archimedes method. The theoretical density (ρ_x) of the ceramics was obtained by using the unit

P. Liu (✉) · W.A. Su · G.G. Yao · X.B. Bian
School of Physics and Information Technology,
Shaanxi Normal University,
Xi'an 710062, China
e-mail: Liupeng68@hotmail.com

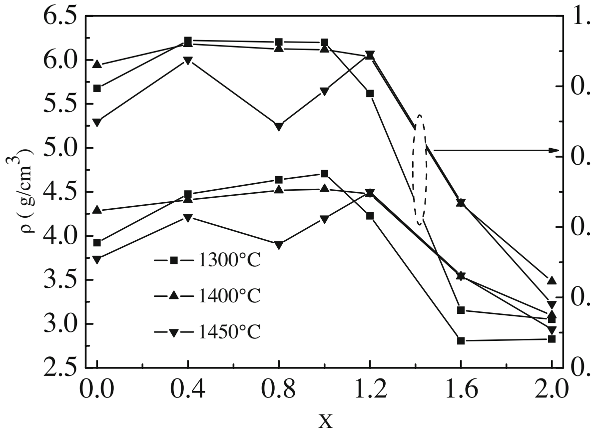

Fig. 1 Bulk density (ρ) and relative density (ρ_r) of $Mg_4(Nb_{2-x}Sb_x)O_9$ ceramics sintered at different temperatures for 5 h

cell dimensions from the XRPD data. The measurement of dielectric constant (ε) and unloaded Q of $Mg_4Nb_2O_9$ ceramics was performed in T_{011} mode at 8–11 GHz by the Hakki-Coleman dielectric resonator method [7] using a network analyzer(Agilent Tech., hp8720ES). The temperature coefficient of resonator frequency (τ_f) was calculated in the temperature between 20–80 °C.

3 Results and discussion

The bulk density (ρ) and relative density (ρ_r) of $Mg_4(Nb_{2-x}Sb_x)O_9$ ceramics sintered at various temperatures as a function of x values are shown in Fig. 1. At the sintering temperature of 1300 °C, relative density ρ_r increased from 0.87 to 0.96 as x values from 0 to 0.4, and then, ρ_r values saturated at $0.4 \le x \le 1.0$. As $x > 1.2$, ρ_r decreased abruptly to 0.57 for $x=1.6$. This demonstrated that Sb^{5+} substitutions for Nb^{5+} is effective in reducing the sintering temperature of $Mg_4(Nb_{2-x}Sb_x)O_9$ for $0.4 \le x \le 1$, but suppressed the densification process as the compositions $x > 1.2$. The present result is also confirmed by the radical shrinkage(s) of $Mg_4(Nb_{2-x}Sb_x)O_9$ ceramics sintered at various temperatures as a function x shown in Fig. 2.

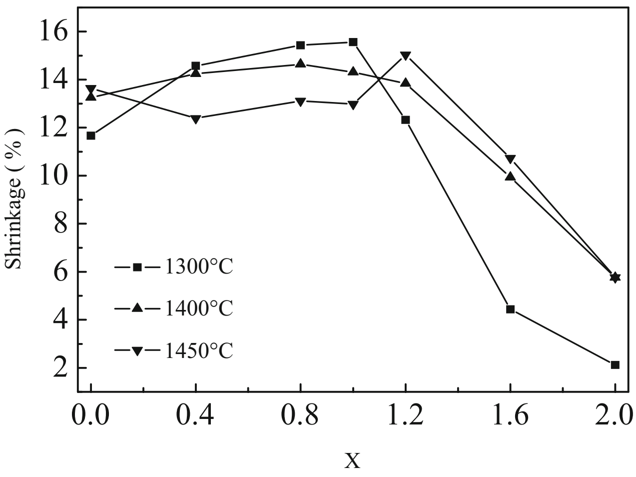

Fig. 2 The shrinkage of $Mg_4(Nb_{2-x}Sb_x)O_9$ ceramics sintered at different temperatures for 5 h

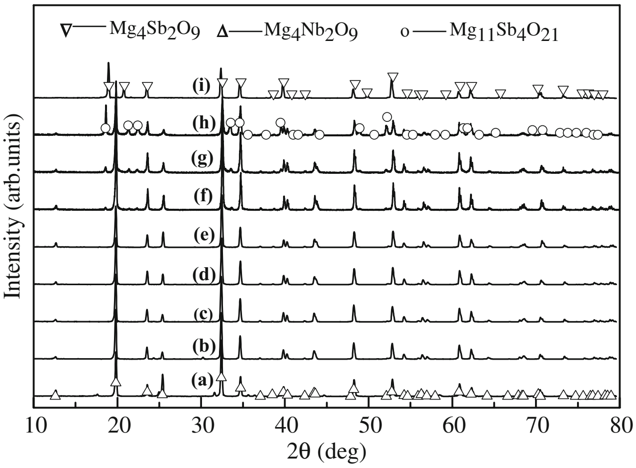

Fig. 3 XRPD patterns of sintered $Mg_4(Nb_{2-x}Sb_x)O_9$ ceramics (**a**) $x=0.4$, (**b**) $x=0.8$, (**c**) $x=1.0$, (**d**) $x=1.2$, (**e**) $x=1.6$, (**f**) $x=1.7$, (**g**) $x=1.8$, (**h**) $x=1.9$, (**i**) $x=2.0$

Figure 3 shows the XRPD patterns of $Mg_4(Nb_{2-x}Sb_x)O_9$ with $0 \le x \le 2$. The formation of impurity phase was not detected in compositions with $x \le 1.6$, and the compounds exhibited the ordered corundum structure of $Mg_4Nb_2O_9$ (JCPDS number: 36-1381) with the space group of $P\overline{3}c1$ (No. 165). As the composition x ranged from 1.7 to 1.9, two phases, i.e. $Mg_4Nb_2O_9$ and $Mg_{11}Sb_4O_{21}$ (JCPDS: 23-0380) were found to be co-exist, as shown in Fig. 3(f), (g), and (h), respectively. As $x=2.0$, the XRPD patterns were indexed as a $Mg_4Sb_2O_9$ phase with the JCPDS number of 23-0378. The lattice parameters, a, c and V, shown in Fig. 4, decreased linearly as the composition x increasing from 0 to 1.6, and

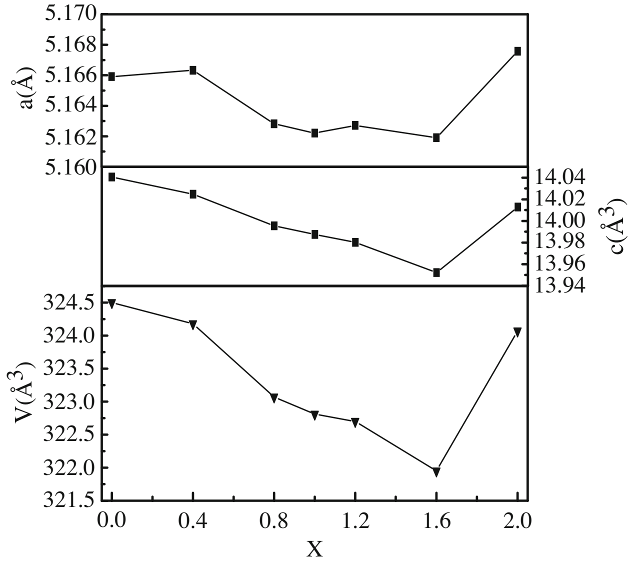

Fig. 4 Lattice parameters, a, c, and unit cell volume V of $Mg_4(Nb_{2-x}Sb_x)O_9$ ceramics

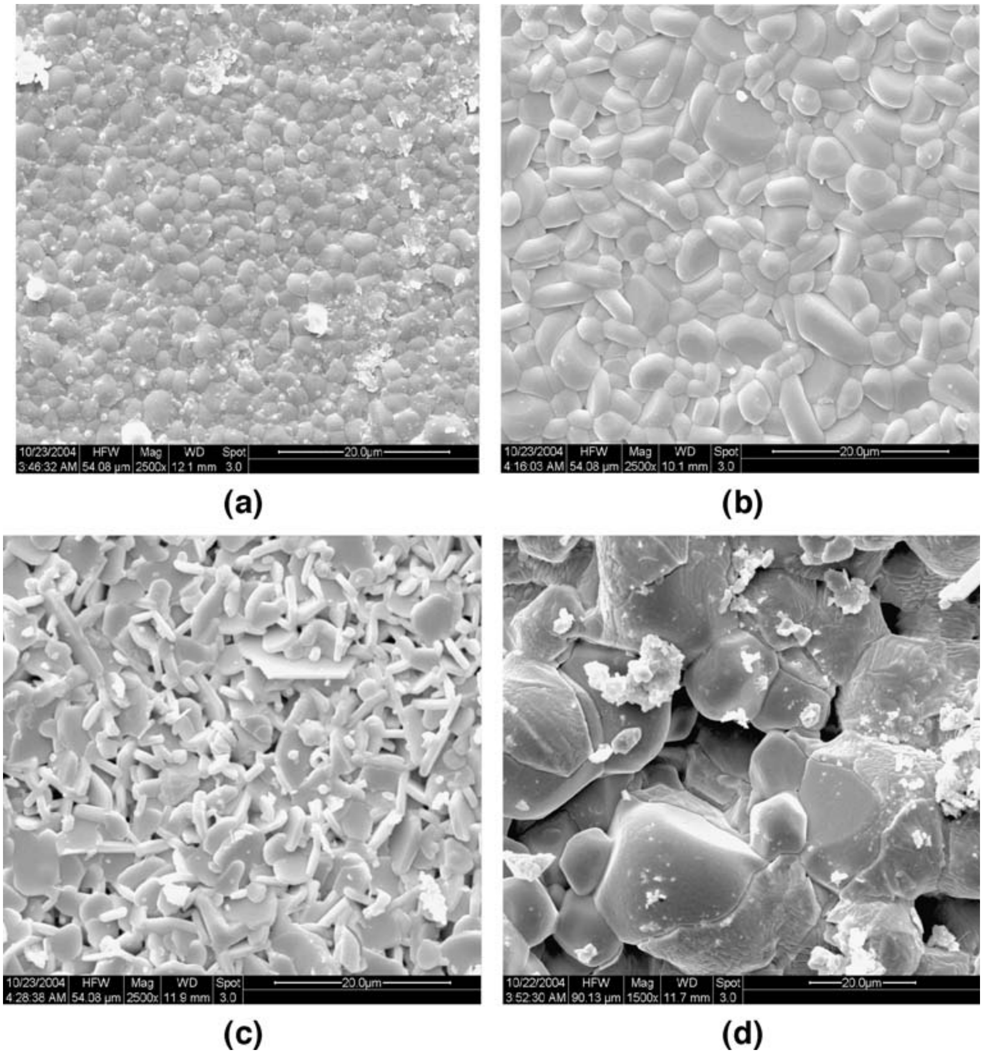

(a) (b) (c) (d)

Fig. 5 SEM micrographs of $Mg_4(Nb_{2-x}Sb_x)O_9$ ceramics sintered at 1300 °C for 5 h: (**a**) x=0.0, (**b**) x=0.8, (**c**) x=2.0, (**d**) x=0.8 sintered at 1450 °C for 5 h

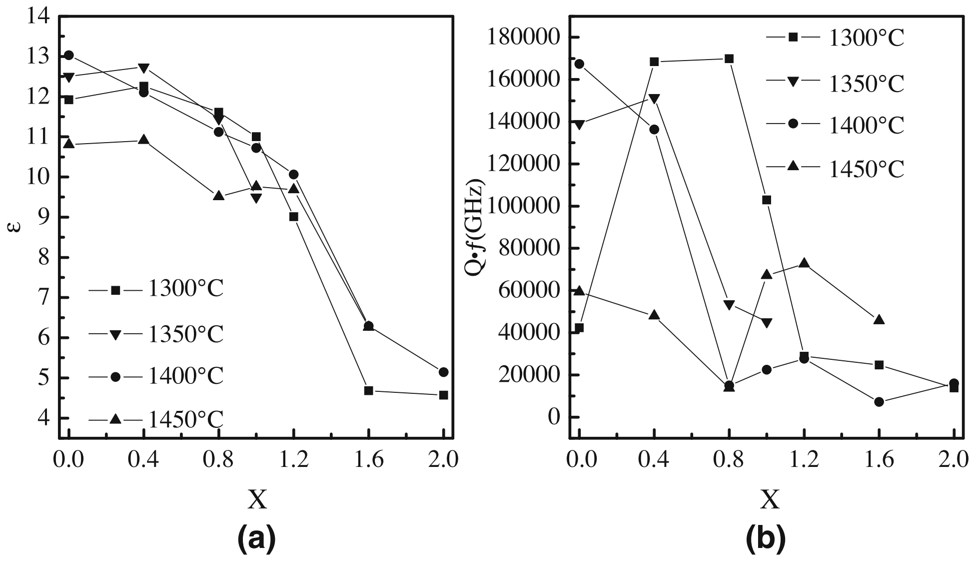

(a) (b)

Fig. 6 The dielectric constant, ε (**a**), quality factor, Qf (**b**), of $Mg_4(Nb_{2-x}Sb_x)O_9$ ceramics sintered at different temperatures

Table 1 The microwave dielectric properties of $Mg_4(Nb_{2-x}Sb_x)O_9$ ceramics sintered at appropriate temperatures.

Composition x	Sintering temperature (°C)	ρ_r (%)	ε	Qf (GHz)	τ_f (ppm/°C)
0	1400	94.4	13.06	162,350	−70.8
0.4	1300	96.0	12.26	168,450	−56.4
0.8	1300	96.1	11.62	169,750	−50.4
1.0	1300	96.3	11.02	92,120	−52.7
1.2	1400	94.7	10.14	33,250	−37.1
1.6	1400	73.2	6.28	8,670	−40.1
2.0	1400	62.1	5.22	13,460	−18.1

then departed from liner relation as $x>1.6$. Thus, the limit of $Mg_4(Nb_{2-x}Sb_x)O_9$ solid solutions is located at composition $x=1.6$, in agreement with reference [8].

Figure 5 shows the surface micrographs of the as-sintered $Mg_4(Nb_{2-x}Sb_x)O_9$ ceramics for $x=0$, 0.8, and 2.0, respectively. As sintered at 1300 °C, the homogeneously fine microstructures were revealed for $Mg_4Nb_2O_9$ ceramics [Fig. 5(a)]. The grain size of this composition is distributed around 0.6–1 μm. For the specimens with $x=0.8$ and sintered at 1300 °C, the dense microstructures without porosity shows the average grain size of about 3 μm [Fig. 5(b)]. As for $x=2.0$, the microstructures of $Mg_4Sb_2O_9$ ceramics shown in Fig. 5(c) are completely packed by plate-like grains isolated by pores. As the sintering temperature increased up to 1450 °C, as shown in Fig. 5(d), the abnormal grain growth was observed for the $Mg_4(Nb_{1.2}Sb_{0.8})O_9$, which is in agreement with an obvious decrease of density shown in Fig. 1.

Figure 6 shows the dielectric constant, ε, and Qf value of $Mg_4(Nb_{2-x}Sb_x)O_9$ ($0\leq x\leq 2$) ceramics as a function of the composition x for various sintering conditions. As shown in Fig. 6(a), the ε values of sintered ceramics decrease from 13.06 to 6.28 as x increases from 0 to 1.6. In Fig. 6(b), the Qf value of $Mg_4(Nb_{2-x}Sb_x)O_9$ ceramics is dependent on the compositions x and sintering temperatures. After sintering at 1300 °C, the Qf values of $Mg_4(Nb_{2-x}Sb_x)O_9$ ceramics increase from 42,000 to 168,450 GHz as the composition x ranges from 0 to 0.4. The Qf values of $Mg_4(Nb_{2-x}Sb_x)O_9$ ceramics with $x=0.4$ and 0.8 sintered at 1300 °C are comparable to those of $Mg_4Nb_2O_9$ ceramics sintered at 1400 °C. However, for $x\geq 1.2$, Sb suppresses the Qf values due to the formation of plate-like grains, pores, abnormal grain growth, and impurity phases mentioned above.

The temperature coefficients of resonant frequency, τ_f of $Mg_4(Nb_{2-x}Sb_x)O_9$ ceramics sintered at appropriate temperatures are given in Table 1. As the composition x increases, the τ_f values increase. The τ_f values of all specimens have shown large negative values. The $Mg_4(Nb_{1.6}Sb_{0.4})O_9$ ceramics sintered at 1300 °C for 5 h has the optimum microwave dielectric properties of $\varepsilon=12.26$, Qf=168 450 GHz (at 8.714 GHz), and $\tau_f=-56.4$ ppm/°C

4 Summary

The $Mg_4(Nb_{2-x}Sb_x)O_9$ ($0\leq x\leq 2$) ceramics were prepared by a conventional solid reaction method. $Mg_4(Nb_{2-x}Sb_x)O_9$ solid solutions with composition x ranging from 0 to 1.6 had the ordered corundum structure of $Mg_4Nb_2O_9$. The lattice parameters, a, c and the volume V of $Mg_4(Nb_{2-x}Sb_x)O_9$ decreased with x as $x\leq 1.6$, whereas, the impurity phase $Mg_{11}Sb_4O_{21}$ appeared as the composition x ranged from 1.7 to 1.9. With a substitution of Sb^{5+} for Nb^{5+} ($0.4\leq x\leq 0.8$), the sintering temperature of $Mg_4Nb_2O_9$ ceramics was reduced from 1400 to 1300 °C without degenerating the Qf values, but the dielectric constant, ε, decreased from 13.06 to 6.28 as x varied from 0 to 1.6. Typically, the $Mg_4(Nb_{1.6}Sb_{0.4})O_9$ ceramics sintered at 1300 °C for 5 h showed the optimum microwave dielectric properties: $\varepsilon=12.26$, Qf=168 450 GHz (at 8.714 GHz), $\tau_f=-56.4$ ppm/°C.

Reference

1. N.M. Alford, S.J. Penn, J. Appl. Phys. **80**, 5895 (1996)
2. T. Tsunooka, M. Androu, Y.Higashida, H. Sugiura, H. Ohsato, J. Eur. Cer. Soc. **23**, 2573 (2003)
3. S.M. Moussa, Appl. Phys. Lett. **82**, 4537 (2003)
4. J-H. Sohn, Jpn. J. Appl. Phys. **33**, 5466 (1994)
5. N. Kumada, K. Taki, N. Kinomura, Mat. Res. Bull. **35**, 1017 (2000)
6. H. Ogawa, A.Kan, A.Ishihara, Y. Higashida, J. Eur. Cer. Soc. **23**, 2485 (2003)
7. B.W. Hakkit, P.D. Coleman, Micr. Theo. Tech. **8**, 402 (1960)
8. A. Yoshida, J. Eur. Cer. Soc. **24**, 1765 (2004)